

Effect of Coiling Temperature on the Microstructure and Mechanical Properties of Hot-Rolled Ti–Nb Microalloyed Ultra High Strength Steel

Pradip K. Patra¹ · Srimanta Sam¹ · Mrigendra Singhai¹ · Sujoy S. Hazra² · G. D. Janaki Ram³ · Srinivasa Rao Bakshi³

Received: 2 August 2016 / Accepted: 14 October 2016 / Published online: 4 November 2016
© The Indian Institute of Metals - IIM 2016

Abstract A novel low carbon Ti–Nb microalloyed hot rolled steel with minimum yield strength of 700 MPa and good balance of stretch-flangeability and impact toughness has been developed by controlled thermo-mechanical processing following thin slab direct rolling route. In the present work, the effects of two coiling temperatures on the resulting microstructure, micro-texture and mechanical properties on this Ti–Nb microalloyed steel have been studied. It is observed that increase in coiling temperature from 520 to 580 °C significantly affects the mechanical properties. Higher dislocation density and increased precipitation along with slightly smaller grain size is observed for 580 °C coiling temperature resulting in about 50 MPa increase in yield and tensile strengths as compared to 520 °C coiling temperature.

Keywords Microalloyed · High strength · Ti–Nb steel · Precipitation strengthening · Hot rolled · Coiling temperature

1 Introduction

Lighter weight vehicle for reducing CO₂ emissions and increased passenger safety in terms of better crash worthiness have necessitated the need for developing hot rolled

thin steel sheets with high strength coupled with high elongation for fabrication of automotive structural parts such as long and cross members. In this regard, microalloyed high strength low alloy (HSLA) steels are the most potential solutions due to their ability to achieve final mechanical properties in as rolled condition, thus eliminating the need of heat treatment [1, 2]. Conventionally, hot rolled steels with yield strengths of up to 500 MPa consisting of only ferrite or ferrite and pearlite microstructures have been microalloyed with Nb, Ti and V, individually or in combination such that they are primarily strengthened by solid solution hardening and grain refinement by thermo-mechanical rolling combined with precipitation hardening [1].

The prevailing literature indicates that production of hot rolled high yield strength (YS) steels have been realized based on several alloying concepts [2–4]. Alloying elements like Mn, Nb, V, Ti, Mo, Ni and Cu are commonly added for the production of high strength steels to obtain the desired microstructure and mechanical properties. Mao et al. [5] studied the microstructure and mechanical properties of a high strength grade and a reference grade weather resistant steel (YS = 460 MPa), both produced by a six-stand Compact Strip Production (CSP) mill, focusing on the precipitation behaviour of the titanium carbonitrides and carbides. The chemical composition of investigated high strength steel was 0.05 %C–1.1 %Mn–0.23 %Si–0.12 %Ti–0.007 %N along with weather resisting elements which included 0.25 %Cu, 0.55 %Cr and 0.15 %Ni; the reference grade differed in Ti content, which was kept at 0.016 %. Both types of steels were cast into a thin slab caster with slab thickness of 60 mm which was then directly charged into a tunnel furnace and soaked for 20 min at 1150 °C before tandem rolling into final thickness of 2–6 mm. The finish rolling temperature and coiling temperature were controlled at 880

✉ Pradip K. Patra
pradip.patra@jsw.in

¹ JSW Steel Ltd., Dolvi Works, Dolvi, Taluka - Pen, Maharashtra 402107, India

² Ferro Tech India Pvt. Ltd., Mumbai 400013, India

³ Department of Metallurgical and Materials Engineering, Indian Institute of Technology Madras, Chennai 600036, India

and 600 °C respectively. The microstructure of high strength steel was inhomogeneous and composed of quasi-polygonal ferrite grains of 3.3 µm average size having a high dislocation density and large number of 5–10 nm sized TiC (mostly) precipitates resulting in high strength (YS = 700 MPa). Yi et al. [6] investigated a high strength low carbon steel having composition of 0.081 %C–1.74 %Mn–0.10 %Si–0.18 %Ti and YS of 700 MPa, with the help of laboratory-scale thermo-mechanical simulations. Using CCT curves (with and without strain of 0.4), they showed that hot deformation accelerated ferrite and pearlite transformations while retarding bainite transformation. The formation of high density defects in the austenite suppressed the bainite transformation, especially when a sub-grain structure was formed in austenite as a result of hot deformation. It was found that increased cooling rate from finish rolling temperature to coiling temperature increased the bainite fraction from 10 to 90 % resulting in increased strength and concurrent decrease in total elongation from 26 to 20 %. TEM studies indicated that the high strength was due to the tiny interlocked distribution of bainitic ferrite laths and dispersion of fine TiC precipitates. Wang et al. [7] have utilised Ti–Nb concept to produce high strength steel with YS of 710–790 MPa range and total elongation of 19 %. The experimental steel of composition 0.11 %C–1.95 %Mn–0.2 %Si–0.12 %Ti–0.08 %Nb–0.004 %N in wt% was hot rolled to 5 mm thickness, in a 2-high reversing rolling mill, by reheating at 1270 °C and rolling at 950 °C, followed by cooling at a rate of 15 °C/s to the coiling temperature of 550 °C, followed by water quenching. The isothermal precipitation behaviour was further studied in the range 400 °C to 650 °C, and it was observed that a large number of <10 nm (Nb, Ti)C precipitate, dispersed in the ferrite or bainitic ferrite matrix, resulted in significantly improved strength of steel. Based on Ti–Mo alloying concepts, Funakawa et al. developed a new class of hot rolled 740 MPa YS steel with excellent stretch flange formability by precipitation of nanometer sized carbides and also by preventing large cementite and pearlite formation [8]. The steels had a base composition of 0.04 %C–1.5 %Mn–0.2 %Mo with varying levels of Ti (0.012–0.18 %), such that the small amount of Mo retarded the formation of both pearlite and large cementite at grain boundaries. A UTS value of 800 MPa was successfully achieved with 0.1 %Ti addition with almost all the carbon being consumed to form 3 nm sized TiC precipitates.

The above mentioned few reports indicate that for developing low carbon steels with YS more than 700 MPa, grain refinement as well as precipitation hardening must play prominent roles. In this regard, the microstructures and mechanical properties of the hot rolled strips are known to be greatly influenced by the coiling temperatures, apart from rolling reductions, finish rolling temperatures and cooling rates on the run-out-table (ROT) [9, 10]. With the coiling

temperatures being closely associated with the precipitation of major microalloying elements like Nb, Ti and Mo, its precise control is of paramount importance to utilise the maximum potential of precipitation strengthening and minimize variation in mechanical properties of hot rolled coils. However, reports dealing with optimisation of coiling temperatures in these high strength hot rolled strips are relatively scarce.

In the present study, a low carbon high strength Ti–Nb microalloyed steel has been industrially produced at the CSP mill of JSW Steel's Dolvi works in India. The steel has been coiled at two different temperatures and the effect of the resultant microstructure on the mechanical properties (tensile, stretch-flange ability and impact toughness) has been studied.

2 Experimental

2.1 Preparation of Hot Strips

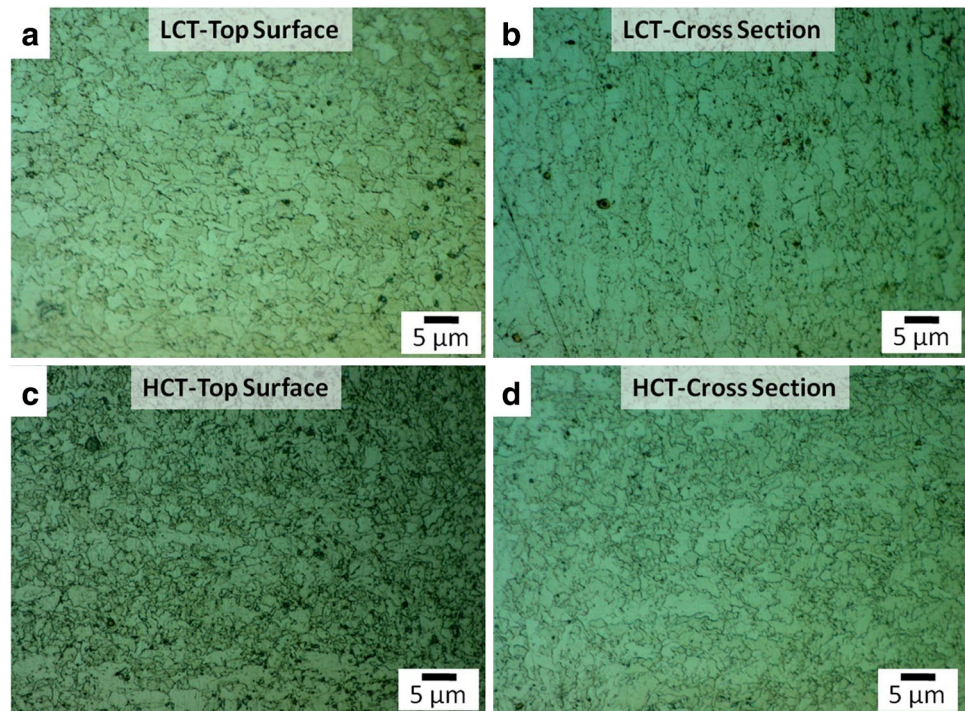
The industrial heat was produced in a 200 MT Electric Arc Furnace (CONARC) and the final chemistry was adjusted in Ladle Furnace (LF) station. The liquid metal was casted into 1250 mm width and 62 mm thick slab in a CSP caster. The Compact Strip Production process is a combination of the thin slab casting and direct rolling processes. The thin slab (50–70 mm thick) from CSP was first descaled, sheared to the desired length and then transported at 960–970 °C to a RLNG fired soaking furnace set between 1110 and 1150 °C where it was soaked for 15–25 min. The slab was again descaled and hot-rolled using a 6-stand hot rolling mill to 6 mm thick plates. The hot strips exited the mill at temperatures between 800 and 900 °C in the austenitic condition and were then cooled on the run-out table with water spray before being coiled at specific temperature. In the present study, two strips were produced; one at lower coiling temperature of 520 °C (named LCT sample) and the other at higher temperature of 580 °C (named HCT sample). These temperatures were chosen based on the usual coiling temperature range of 500–600 °C. Excessive temperatures might lead to oxidation, decarburization and grain growth. Also, as the work was done in industrial scale, too much experimentation was not possible. The composition of the steel prepared at JSW Dolvi Works is provided in Table 1. Table 1 indicates that it was a low C, moderate Mn steel with Nb and Ti as microalloying elements. The steel had a much high Ti:N ratio (~16) than the stoichiometry for TiN (3.42).

2.2 Microstructural Characterization

Optical microscopy was carried out on the longitudinal and transverse section of the sheets. Samples were prepared using standard metallographic procedure and etched using

Table 1 Composition of the steel

Element	C	Mn	Si	S	P	Al	N	Nb	Ti	Fe
wt%	0.045	1.58	0.25	0.004	0.01	0.038	0.0072	0.0063	0.12	Bal.

Fig. 1 Optical microscopy images of the top surface and cross section of the LCT and HCT samples

2 % Nital solution. Transmission electron microscopy was carried out using a Tecnai T20 TEM for which samples were prepared using an ion milling equipment. EBSD scans were carried on electro-polished surfaces ($\sim 500 \mu\text{m} \times 500 \mu\text{m}$) with the help of TSL-OIM system attached to FEI Quanta 200 HV W-filament SEM. The step size was kept at $0.4 \mu\text{m}$. While post-processing the EBSD scan data, only measurement points with confidence index more than 0.1 were further considered, such that for misorientation analyses and grain size estimations, misorientations below 2° were ignored. Further, misorientation angles of 2 and 15° were imposed for delineating low and high angle grain boundaries (LAGBs and HAGBs) respectively, such that grains were considered to consist of minimum 15 pixels.

2.3 Mechanical Property Measurements

The hardness was measured using a micro Vickers hardness tester (Model 420 MVD, Wolpert Wilson Instruments, USA) with a 10 s dwell time and a load of 500 g. Quasi-static uniaxial tensile tests were carried out on a servo-hydraulic Instron tensile testing machine fitted with video extensometer as per ASTM E8. The yield strength, ultimate tensile strength, % elongation until UTS and total % elongation were measured from the curve and reported.

Stretch flange formability was evaluated by the Hole Expansion Test as per the ISO 16630:2009. A 100 mm square sheet having a 10 mm diameter hole drilled in the center were used. The hole was expanded by a cylindrical punch until crack appeared at the hole edge. The hole expansion ratio was evaluated using the following formula [11].

$$\%HER = \frac{D_f - D_i}{D_i} \times 100 \quad (1)$$

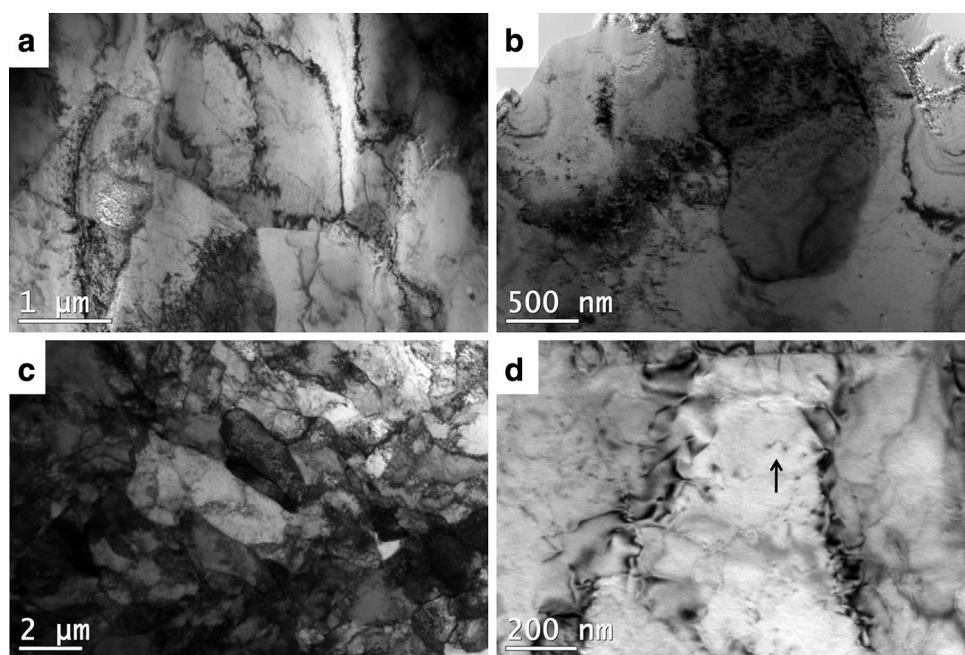
where D_f is the final diameter and D_i is the initial diameter. The impact transition temperature tests were carried out in sub-sized samples as per the ISO 148-1:2009 standard. All the mechanical test result reported were the average of three test results.

3 Results

3.1 Effect of Coiling Temperature on the Microstructure

Figure 1 shows the optical micrographs of the top surface and the cross section of the hot strips. The microstructure consists of polygonal ferrite. It is observed that the LCT samples show a higher grain size compared to the HCT

Fig. 2 Bright field TEM images of LCT (a, b) and HCT (c, d) samples. Nanosized precipitates pinning dislocations can be observed in d



samples. Both the samples have fine grain size below 5 μm . The grain sizes have been measured from EBSD images as explained in later section. It is also observed the HCT samples have slightly smaller grain size compared to LCT samples.

Figure 2 shows the TEM images of the samples. The samples have been prepared parallel to the strip surface. It is clearly observed that the HCT samples exhibit finer grain size than LCT samples. Well formed grains of polygonal ferrite are observed in the LCT samples. Figure 2 shows deformed grains in HCT sample, resulting from high temperature coiling deformation. Pinning of dislocations by nanosized precipitates can also be observed in Fig. 2d. These precipitates are known to be of the type (Ti, Nb)C [12–14] in advanced high strength steels containing Ti, Nb and N. Misra et al. have mentioned that, the most of the precipitation of Nb and Ti carbides take place in the austenitic phase which prevents recrystallization of the austenite during hot rolling. This results in very fine grained polygonal ferrite upon cooling. The precipitation takes place throughout the cooling phase up to coiling. The finest precipitates are formed during coiling [9, 14]. Misra et al. [9] have characterized the precipitates in these type of steels as four types: 1–1.5 μm intergranular rod-like (Fe, Mn)₃C; 120–400 nm Cuboid, round, oblong, or ellipsoidal (Ti, Nb)N; 10–120 nm spherical or plate type (Nb, Ti)C and 3–5 nm needle-like (Nb, Ti)C. The present investigation does not reveal any (Fe, Mn)₃C type precipitates, but (Ti, Nb)N and (Nb, Ti)C type precipitates are observed. Further characterization can be done using a 3D Atom Probe. The size and number density of the precipitates has been found

to be relatively higher in HCT samples. This is due to the high temperature and low cooling rates (in case of HCT sample) which promotes diffusion and precipitation. It is noted that the slower cooling rate and higher temperature in HCT sample also results in lower driving force for nucleation. Thus the overall effect is observed as a small increase in precipitate density in HCT compared to LCT sample. Lower coiling temperature is achieved by higher cooling rate of the strip after the finishing mill. These precipitates are expected to inhibit grain growth and contribute towards precipitation strengthening as is well known in case of HSLA steels [15]. The relatively lower amount of the precipitates in LCT samples lead to slightly larger grain size. These lower precipitation and larger grain size are expected to result in lower strengthening in case of LCT sample compared to HCT sample.

Figure 3 shows the EDS data taken from a precipitate in TEM showing the peaks corresponding Ti, C and Nb being present in addition to Fe (from matrix). This confirms that these precipitates are of the type (Ti, Nb)C, although exact composition cannot be determined from EDS. More accurate studies using 3D Atom Probe are required in order confirm the composition of these precipitates.

3.2 Electron Backscatter Diffraction (EBSD) Imaging

Figure 4 shows the EBSD [001] inverse pole figure images of the samples. It is clearly seen that the grain size is very fine, less than 5 μm . Figure 5 shows the grain size distribution and the distribution of the grain misorientation angle. With increase in CT from 520 to 580 $^{\circ}\text{C}$, minor

Fig. 3 TEM EDS data taken from a precipitate showing presence of Ti, Nb and C

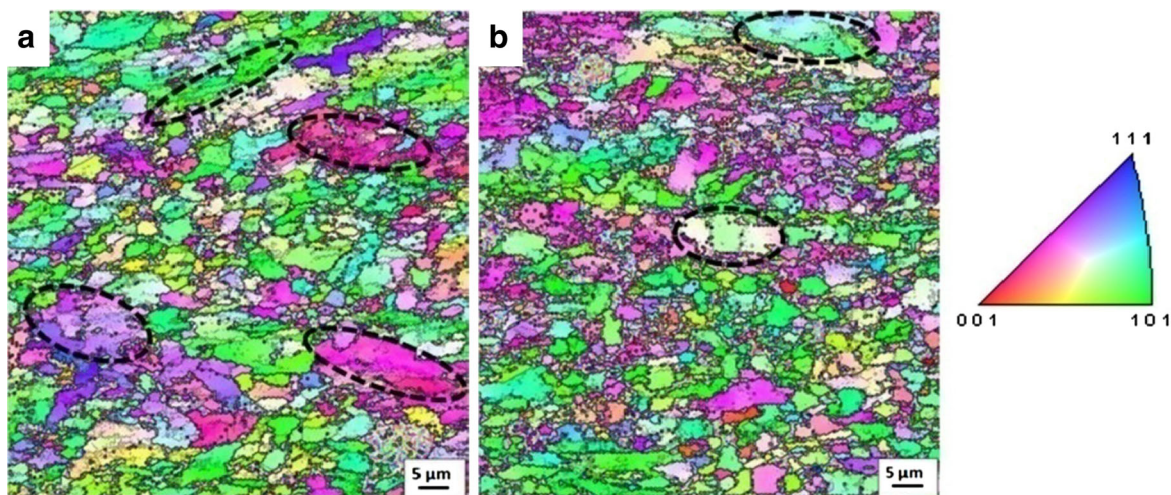
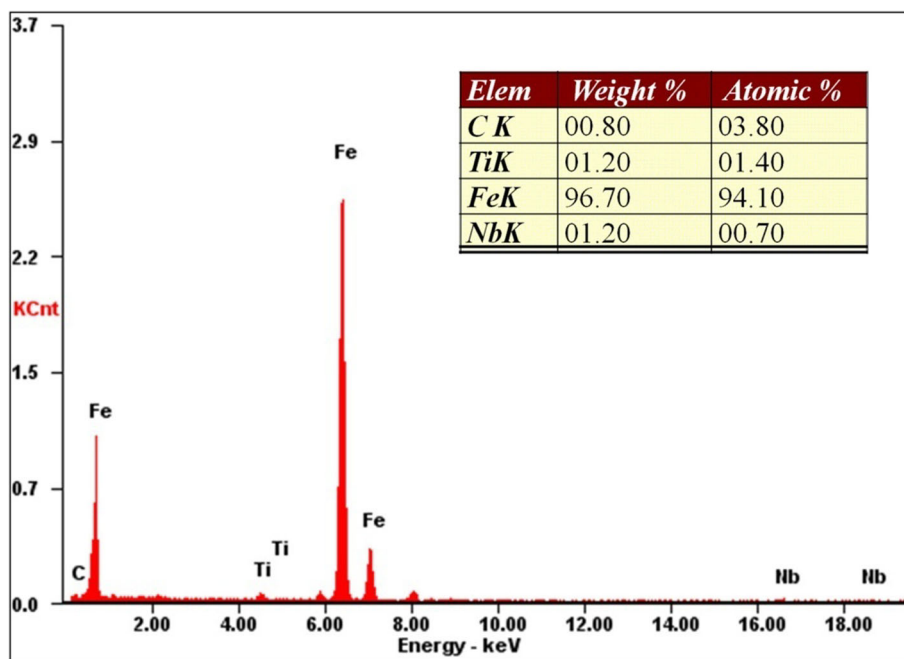


Fig. 4 EBSD [001] inverse pole figure image of **a** LCT and **b** HCT samples

refinement in grain size in addition to a reduced width of distribution can be clearly observed. The average grain size reduces from 3.9 to 3.5 μm with increase in coiling temperature. There is a reduction in low angle grain boundaries (LAGB) fraction from ~ 23 to $\sim 16\%$ with increase in coiling temperature. The higher area fraction of larger sized grains for lower CT sample as reflected in Fig. 5a is also in concurrence with more microstructural heterogeneities noted in Fig. 4a.

It may however be noted that the effect of change in CT on the final ideal BCC texture components (i.e. α -fibre, represented by $\langle 110 \rangle$ ||RD and γ -fibre, represented by $\langle 111 \rangle$ ||ND) as evidenced by the $\{110\}$ Pole

Figure Maps (Fig. 6) and the $\phi_2 = 45^\circ$ sections of ODFs for the two steels (Fig. 7), is trivial in nature. A pronounced α -fibre with highest intensities at $(112) \langle 110 \rangle$ and $(223) \langle 110 \rangle$ is present with not-so-weak α -fibre components of $(554) \langle 112 \rangle$ in both the cases, which is in concurrence with expected hot rolled texture evolution in micro-alloyed steels [16]. It is noted that the deformation takes place in austenite phase only and the transformation to ferrite results during cooling on the run-out table which results in this transformation texture. It is very commonly observed in ferrite and ferrite/pearlite obtained by air cooling of hot rolled austenite as mentioned by Hutchinson et al. [17].

Fig. 5 Variation of the grain size and misorientation angle from EBSD data analysis

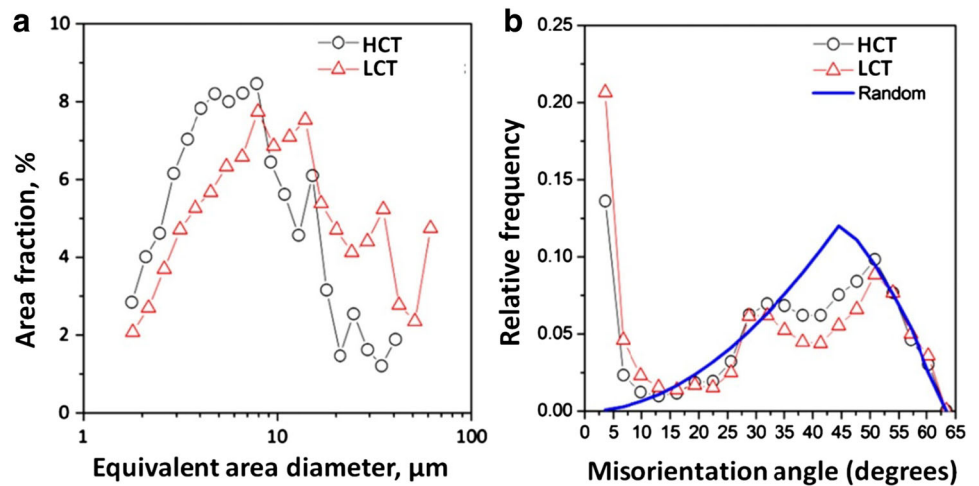
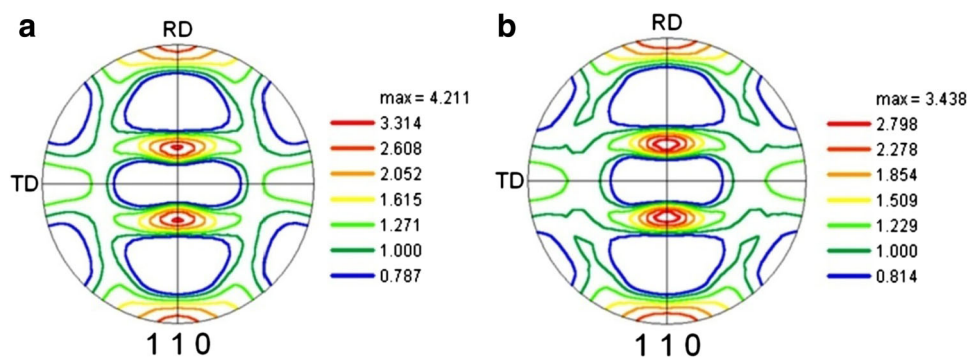


Fig. 6 EBSD-based {110} pole figures: **a** LCT and **b** HCT sample



3.3 Mechanical Properties

Figure 8 shows the stress strain curve for the samples. The mechanical properties of the sample measured from microhardness and tensile test are presented in Table 2.

A yield strength of more than 700 MPa and ultimate tensile strength above 750 MPa can be achieved in the HCT sample. The strength and elongation characteristics indicate that the LCT sample meet the mechanical property requirements of standard EN 10149 S650MC grade, whereas HCT sample meet the requirement of standard EN 10149 S700MC grade. It is observed that the HCT sample shows better mechanical properties. The hardness also is observed to be in tune with the mechanical property variation. The % elongation is found to be reasonably good and on par with HSLA steels. The Charpy impact tests indicate that the HCT sample is tougher compared to LCT sample. The HCT sample shows a hole expansion ratio (HER) value of 114 % which is similar to mild steel. The LCT sample has higher HER value indicating better stretch formability. It is known that presence of hard phases such as martensite can reduce the HER as in case of Dual phase steel despite of high elongation [11]. The difference in hardness between ferrite and martensite in dual phase steel

affects the micro void formation and crack propagation during hole expansion test [18, 19] Whereas in single phase bainite steel, HER value is high but the elongation is low [20]. The high HER value obtained in this steel is mainly due ferrite dominated microstructure.

4 Discussion

4.1 Effect of Coiling Temperature on Microstructure

The optical micrographs in Fig. 1 and EBSD images in Fig. 4 clearly indicate that the microstructure consists of polygonal ferrite grains. It is also observed that the HCT sample has a slightly finer grain size. The TEM images in Fig. 2 further confirm the fine grain size and increased presence of precipitates in HCT sample. The increased precipitation in case of HCT sample can be attributed to slower cooling rate as well as higher temperatures at any instant compared to LCT sample. This is expected to result in increased diffusion of carbon in HCT samples. The enhanced precipitation leads to pinning of grain boundaries thereby reducing the grain growth and explains the smaller

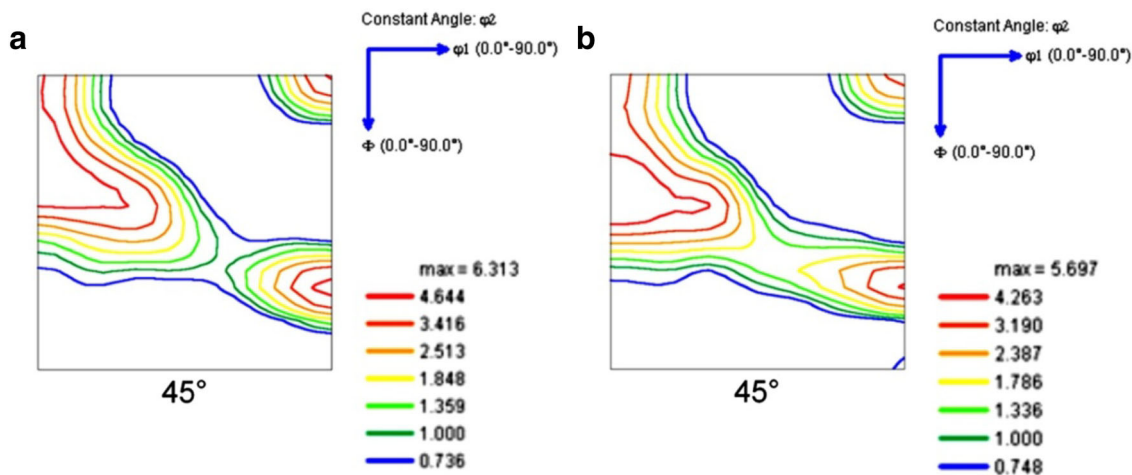


Fig. 7 $\phi_2 = 45^\circ$ section of EBSD-based ODF calculated for: a LCT and b HCT sample

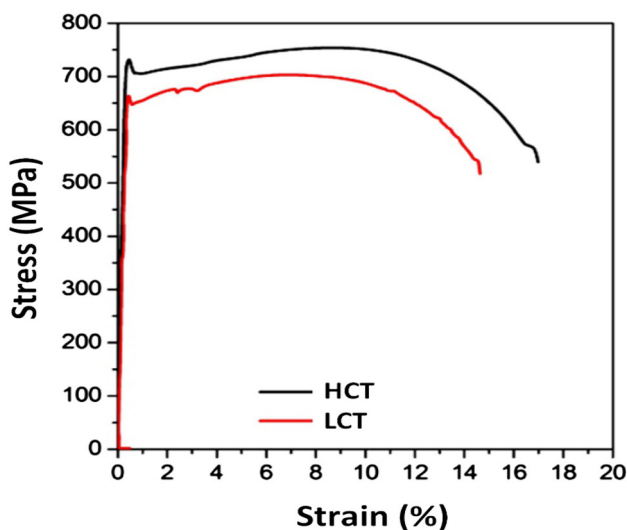


Fig. 8 Engineering stress strain curve for the LCT and HCT samples

grain size in HCT samples. It is observed from the current studies that the coiling temperature can have significant effect on the microstructure.

4.2 Strengthening Mechanisms in Nb–Ti Modified Steels

It is observed that the difference between the YS of LCT and HCT sample is about 60 MPa. This can be explained

based on the various strengthening mechanisms present in micro-alloyed steels such as solid solution strengthening, grain boundary strengthening, dislocation strengthening and precipitation hardening [5, 15, 21]. Patel et al. have observed that grain size refinement ($\sim 40\%$) is a dominant strengthening mechanism followed by dislocation hardening ($\sim 22\%$), precipitation hardening ($\sim 17\%$) and solid solution hardening ($\sim 15\%$) respectively in these steels [22]. Mao et al. [5] have summarized the strengthening mechanisms for Ti-microalloyed steel having strength of the order of 700 MPa. The strength of microalloyed steel can be represented by the following equations:

$$\sigma_{YS} = \sigma_0 + \Delta\sigma_{ss} + \Delta\sigma_{gb} + \Delta\sigma_{ppt} + \Delta\sigma_{dis} \tag{2}$$

$$\Delta\sigma_{ss} = 4570[C] + 4570[N] + 37[Mn] + 83[Si] + 470[P] + 38[Cu] + 80[Ti + Nb] + 0[Ni] - 30[Cr] \tag{3}$$

$$\Delta\sigma_{gb} = kd^{-1/2} \tag{4}$$

$$\Delta\sigma_{ppt} = \frac{5.9\sqrt{f}}{\bar{x}} \ln\left(\frac{\bar{x}}{2.5 \times 10^{-4}}\right), \quad \text{where } f = \frac{[Ti] V_{TiC}}{100 V_{Fe}} \tag{5}$$

$$\Delta\sigma_{dis} = 100\alpha Gb\sqrt{\rho} \tag{6}$$

Here, σ_{YS} is the yield strength of the steel (MPa), σ_0 is the lattice friction stress ($=48$ MPa), $\Delta\sigma_{ss}$ is solid solution contribution (MPa), $\Delta\sigma_{gb}$ is grain boundary strengthening

Table 2 Mechanical properties of LCT and HCT samples

Sample	Hardness, HV _{0.5}	YS, MPa	UTS, MPa	% Elongation	Charpy impact energy (J)		%HER
					−20 °C	−40 °C	
LCT	226 ± 4	660	712	19	136	112	125
HCT	253 ± 6	720	762	20	200	144	114

contribution (MPa), $\Delta\sigma_{\text{ppt}}$ is precipitation strengthening contribution (MPa), $\Delta\sigma_{\text{dis}}$ is the dislocation strengthening contribution (MPa), the element in square brackets represents its weight percent, k is the Hall–Petch coefficient ($=17 \text{ MPa m}^{1/2}$), d is the grain size (m), f is the volume fraction of (Ti, Nb)C precipitates, \bar{r} is the average radius of the precipitates (μm), V refers to specific volume ($=1/\text{density, m}^3/\text{kg}$), α is a constant ($=0.38$), G is shear modulus ($=8.3 \times 10^4 \text{ MPa}$), b is the Burgers vector ($=0.24 \text{ nm}$) and ρ is the dislocation density (m^{-2}).

The solid solution contribution remains the same for both the samples and comes out to be $\sim 337 \text{ MPa}$ for the composition. The grain boundary strengthening contribution turns out to be 71 and 84 MPa respectively for the LCT and HCT samples (increase of 13 MPa). Considering precipitation to be complete in HCT samples, the volume fraction (f) from Eq. (5) turns out to be $(0.12/100) \times (7.8/4.98) = 0.0019$. This corresponds to a strengthening of 27 MPa for 50 nm inter particle distance and 142 MPa for 10 nm inter particle distance. The precipitation of C from the matrix is expected to lower the strength of the HCT sample by some value as well. Mao et al. [5] have also observed the precipitation hardening from TiC precipitates as a dominant factor responsible for a yield strength increment of approximately 158 MPa. It is generally considered that measurement of dislocation density is tedious and often inaccurate. Hence, in most cases, the contribution of dislocation strengthening is usually obtained by subtracting all other contributions from the measured strength value. Since annealed steel has a dislocation density of about $4 \times 10^{10} \text{ m}^{-2}$ [23] we can assume the dislocation density in the hot rolled steels to be of the order of 10^{11} m^{-2} , which results in a strengthening effect of about 240 MPa as per Eq. (6). The small change in the dislocation density between LCT and HCT samples indicate a small difference in strength of the samples due to this contribution. It is seen that σ_{YS} is calculated using Eq. (2) and the calculated values comes out to be in the range of 700–800 MPa. Thus, the 60 MPa increase in the yield strength of HCT sample can be attributed to the small contributions from Hall–Petch effect, precipitation strengthening and dislocation strengthening.

5 Conclusions

A Nb–Ti based hot rolled high strength steel with YS 720 MPa and UTS 760 MPa, with total elongation 20 % was successfully prepared at JSW Steel. The following conclusion could be drawn from the present study.

1. The microstructure of hot rolled Ti–Nb microalloyed steel consisted mainly of quasi-polygonal ferrite. The average grain size was below 4 μm .

2. High temperature coiled samples showed a 60 MPa increase in YS and 50 MPa increase in UTS compared to the low temperature coiled sample.
3. High stretch flange formability and high Charpy impact energy values were observed for both the Ti–Nb micro-alloyed steel.
4. Sample coiled at 580 °C showed a little finer grain size, little higher dislocation density and slightly higher precipitation of (Ti, Nb)C, compared to sample coiled at 520 °C. This could be explained based on higher temperature and slower cooling rates which led to additional time for diffusion of carbon.
5. The increase in strength of the high temperature coiled sample could be explained based on small contributions from grain refinement and precipitation hardening.

References

1. Pickering F B, in *Materials Science and Technology—A Comprehensive Treatment Vol. 7*, (eds) Cahn R W, Haasen P, Kramer E J, VCH, Weinheim (1992), p 349.
2. Gomez M, and Medina S F, *Int. J. Mater. Res.* **102** (2011) 1197.
3. Kuziak R, Kawalla R, and Waengler S, *Arch. Civil Mech. Eng.* **8** (2008) 103.
4. Hazra S S, *Iron Steel Rev.* **56** (2013) 150.
5. Mao X, Huo X, and Sun X, *J. Mater. Proc. Technol.* **210** (2010) 1660.
6. Yi H L, Du L X, and Wang, G D, *ISIJ Int.* **46** (2006) 754.
7. Wang X, Zhao Y, Liang B, Du L, and Di X, *Steel Res. Int.* **83** (2012) 1.
8. Funakawa Y, Shiozaki T, Tomita K, Yamamoto T, and Maeda E, *ISIJ Int.* **44** (2004) 1945.
9. Misra R D K, Nathani H, Hartmann J E, and Siciliano F, *Mater. Sci. Eng. A* **394** (2005) 339.
10. Zhao R J, Fu J X, Wu Y X, Yang Y J, Zhu YY, and Zhang M, *ISIJ Int.* **55** (2015) 1816.
11. X. Fang, Z. Fan, B. Ralph, P. Evans and R. Underhill, *J. Mater. Sci.* **38** (2003) 3877.
12. Lakshmanan V K, and Kirkaldy J S, *Metall. Trans. A* **15** (1984) 541.
13. Houghton D C, *Acta Metall. Mater.* **41** (1993) 2993.
14. Shanmugam S, Tanniru M, Misra R D K, Panda D, and Jansto S, *Mater. Sci. Technol.* **21** (2005) 165.
15. DeArdo A J, Hua M J, Cho K G, and Garcia C I, *Mater. Sci. Technol.* **25** (2009) 1074.
16. Ghosh P, Ray R K, Ghosh C, and Bhattacharjee D. *Scr. Mater.* **58** (2008) 939.
17. Hutchinson B, Ryde L, and Bate P. *Mater. Sci. Forum* **495–497** (2005) 1141.
18. Chen X, Jiang H. Cui Z, Lian C, and Lu C. *Proc. Eng.* **81** (2014) 718.
19. Paul S K, Mukherjee M, Kundu S, and Chandra S, *Comput. Mater. Sci.* **89** (2014) 189.
20. Hairer F, Kremaszky C, Tsipouridis P, and Werner E, in *Proceeding of Materials Science and Technology (MS&T) Conference and Exhibition 2009*, 1391.
21. Cao J, Yong Q, Liu Q, and Sun X, *J. Mater. Sci.* **42** (2007) 10080.

22. Patel J, Klinkenberg C, and Hulka K, in *Proceedings of the International Symposium on Niobium Science & Technology* 2001, 647.
23. Lenard J G, Pietrzyk M, and Cser L, in *Mathematical and Physical Simulation of the Properties of Hot Rolled Products*, Elsevier Science Ltd., Oxford (1999) p 174.